

**UNIVERSITY OF MINNESOTA
SOLAR VEHICLE PROJECT**



**MECHANICAL SYSTEMS STRUCTURAL
REPORT**

January 15, 2010

Project Advisor

Jeff Hammer

Mechanical Team Members

Brakes Team

Bryan Horvat
Rebecca Michels
Jin Yan

Chassis Team

Konrad Brown
Jessica Gilbertson
Sarah Gilbertson
Alex LaMoore

Front Suspension Team

Derek Brochu
Taylor Hill
Dan Nigon
Jon Olson

Rear Suspension Team

Jason Davis
Will Jaffray
Daniel Valencia

Steering Team

Jesse Behnke
Michael Lind
Jon Walberg

Table of Contents

Introduction	3
Chassis / Roll Cage	4
Impact Analysis	9
Brakes	15
Front Suspension	16
Rear Suspension	19
Steering	21
Appendix	
Chassis	23
Front Suspension	24
Rear Suspension	26

1 – Introduction/Overview

Since 1990, the University of Minnesota Solar Vehicle Project (UMNSVP) has produced eight world-class race vehicles. The newest car, Centaurus II, maintains the upright driver seating position introduced in the previous car while utilizing design innovations that optimize this layout.

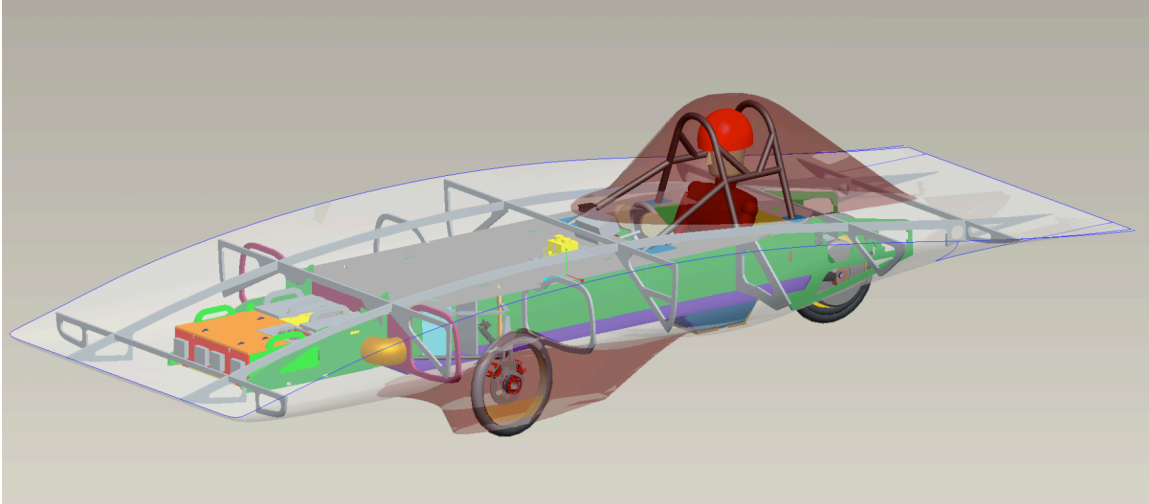


Image 1.1, CAD Image of Vehicle Layout

The upright seating position used in the previous car improved visibility for the driver and increased crush space at the rear of the car. A new chassis design for Centaurus II maintains this seating position, while improving the CG of an upright seating layout and allowing for increased ground clearance and ample crush space. Fiberglass panels were used to construct this chassis due to their excellent strength-to-weight ratio, fracture resistance and electrical resistance over carbon fiber.

The suspension system has been modified to accommodate the higher ground clearance while maintaining excellent stability and minimizing tire scrub. The steering system has been designed to allow the driver more freedom of movement for safer egress and braking over the previous car. The braking and rear suspension systems are based on concepts proven reliable in previous UMNSVP cars, optimized for the Centaurus II layout.

It is the intent of this report to document the features of these mechanical systems and the engineering design and analysis utilized in their development. This report will demonstrate to NASC race officials that our entry is a safe, road-worthy, and competitive vehicle. Any questions or concerns regarding the content of this report may be addressed to either our mechanical team lead or faculty advisor.

Taylor Hill,
Mechanical Team Lead

2 – Chassis and Roll Cage

2.1 - Introduction

Continuing with the University of Minnesota's tradition of building composite chassis', Centaurus II's chassis is constructed from a fiberglass composite. The composite frame accounts for roughly 30 [lbs] of the total vehicle weight of 600 [lbs]. The battery is mounted at the very front of the car to balance out the weight of the driver being concentrated towards the rear of the car while still allowing for an acceptable center of gravity. In an effort to build a high ground clearance car and decrease the aerodynamic drag, the driver actually sits below the bottom panel of the chassis. This can be seen in Figure 2.1 below. Since the driver sits below the bottom plane of the shell, as an extra precaution, a Kevlar lay-up was done on the inside and outside of the 'butt bucket' area where the driver sits.

Figure 2.1 shows the location of the battery with respect to the driver compartment as well as most of the mechanical systems of the car and how they attach to the composite chassis.

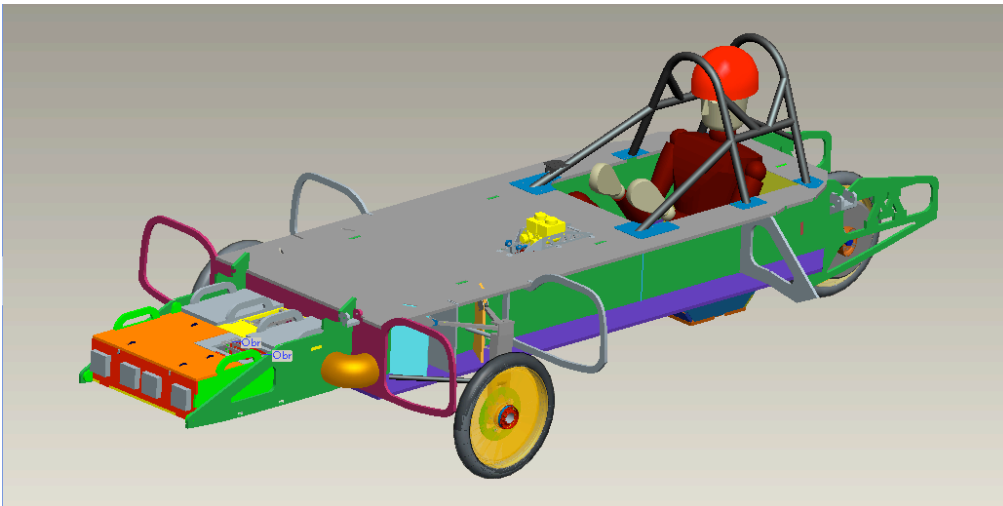


Figure 2.1: Chassis

The chassis includes a composite frame integrated with the bottom of the vehicle shell, suspension components and roll cage. The top shell is completely detachable from the chassis to allow for redirection of the array while the car is stationary. There is also a hinged canopy above the driver compartment to allow for driver egress.

While seated in the driver compartment, the driver is completely isolated from all moving components of the car and the road. The driver compartment contains a 6-point harness, headrest and ventilation system. It was built to allow adequate visibility while driving the vehicle, as well as enough room to allow for safe handling of the vehicle.

2.2 - Mounting to Composite Paneling

Two-part 5319 SERA aluminum inserts (grommets) are used everywhere that requires vehicle components to be fastened to the composite chassis panels. The inserts are designed to handle a bolt-clamping load while distributing shear and axial loads to the composite panel sandwiched between the two parts of the insert. Also, 3M™ Scotch-Weld™ DP-460 NS is used to glue the grommets into the composite paneling, which increases their shear strength dramatically. These inserts have been successfully used on all previous U of M solar vehicles and have been tested on our chassis panels to 1600[lbf] of in-plane shear.

2.3 - Construction

Fiberglass paneling was chosen over Kevlar, carbon fiber and other materials for the chassis mainly because of its high strength to weight ratio and low electrical conductivity. Since fiberglass does not conduct electricity, it makes for an ideal material to attach all of the electrical components of the car to. Also, the composite panels allow for the driver to be completely isolated from all moving parts of the car and the road.

All of the 4.0 [ft.] by 8.0 [ft.] chassis panels were cut down to size using a high-pressure water jet. The panels are assembled in a box-beam geometry with the majority of the panels assembled perpendicular to each other. The panels also have interlocking tabs and slots at all structural joints for improved strength, accurate assembly and consistent high quality joints. A full scale mockup of the chassis and roll bar were constructed to verify driver ingress and egress.

2.4 - Material Specifications

Teklam N505-1 prefabricated fiberglass paneling was used to construct the chassis. The panels have a thickness of 0.50 [in.]. The honeycomb core is made of Nomex with 1/8 [in.] cell diameter. Each side of the core is covered with 1-ply of fiberglass.

The paneling has an average weight of 0.33 [lbs/ft²]. Information was taken from Teklam data sheets and testing procedure documents to determine the maximum allowable stress in the skin of the panels to be 32,970 [psi]. See the appendix A2 for calculations.

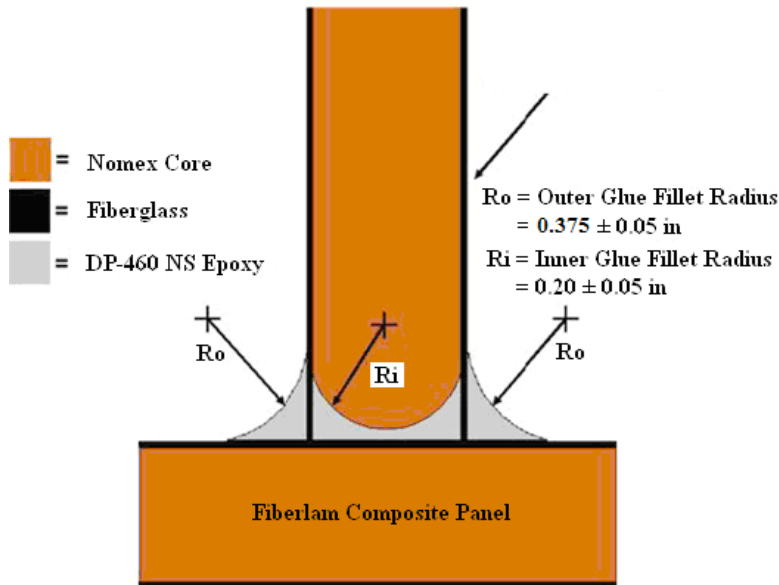


Figure 2.2: DP-460 NS Joint

3M™ Scotch-Weld™ DP-460 NS was used to join all of the chassis panels together. The epoxy is rated at 4900 [psi] under room temperature curing and with the surface preparation conditions used. Typical joints on the car have a shear area per joint inch of 0.5 [in²]. Knowing this, the joint can be assumed to carry a maximum shear load of $(0.5\text{in}) \cdot (4900\text{psi}) = 2450$ [lbf] per inch of joint. See Figure 2.2.

2.5 - Crush Space

NASC regulations require 15 [cm] of horizontal distance between the driver's shoulders, hips and feet and the cars outermost surface. The minimum crush space of Centaurus II is 24 [in]. In a rear collision, there would be 60 [in] of crush space from the trailing edge of the shell to the back of the driver compartment. In the event of a side collision, the driver resides in the center 22 [in] of the total 70 [in] wide car leaving 24 [in] of crush space on either side of the driver compartment. During a front collision, having the battery at the very front of the car helps block penetrating objects as well as decelerates the impacting body due to its mass. In addition, there is 80 [in] of crush space from the leading edge of the car to the driver's feet.

2.6 - Driver Compartment

The driver compartment was designed to be 22 [in] wide in order to allow the driver to move freely enough to safely handle the car while driving, but also to keep them from shifting excessively in the event of an impact. The chassis top panel is located 18 [in] above where the driver actually sits. This would be beneficial in the event of a crash because the majority of the driver's body is encompassed in the structural chassis panels. The driver's shoulders and head are the only parts of the driver outside of the chassis, both of which are protected by the roll cage, which is mounted to the top panel of the chassis.

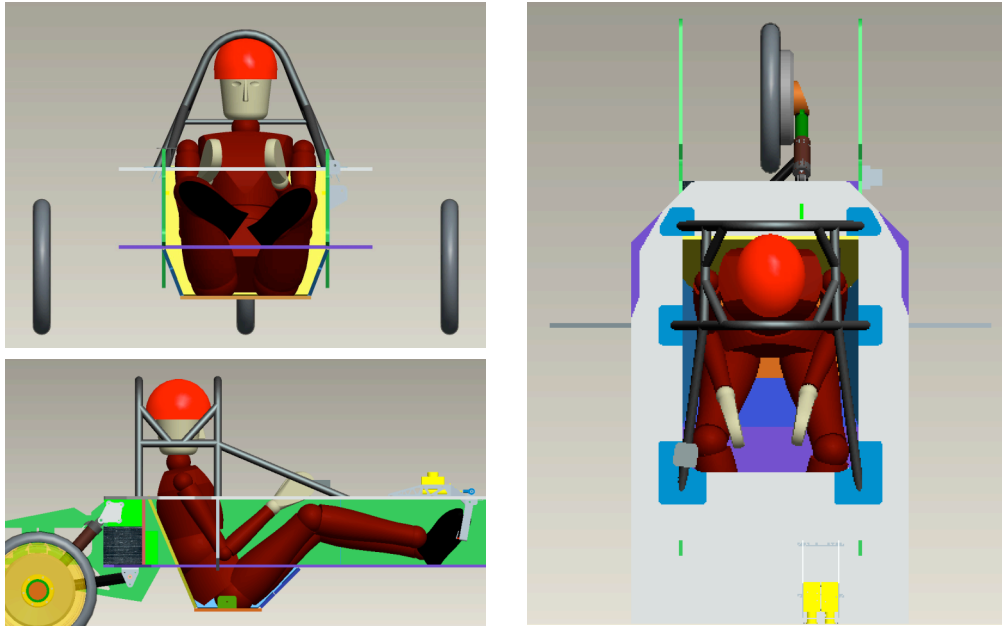


Figure 2.3: Driver compartment: Front, Side and Top Views

2.7 - Safety Harness

A 6-point safety harness is installed into the driver compartment in order to protect the driver in case of a collision. The rear harness attachment points are to a horizontal tube (see Figure 2.3) that is integrated into the roll cage as a part of the rear roll hoop. The seat back is reclined such that it abides by the 27 degree maximum driver seating angle. The front harness attachment points are at the very bottom of the driver compartment positioned so that the belt crosses the driver's hips. This attachment point is part of an angled bracket that is installed via grommets to both the bottom panel and the side panel of where the driver is seated (seen as a small green bracket in Figure 2.3 – side view)

2.8 - Roll Cage

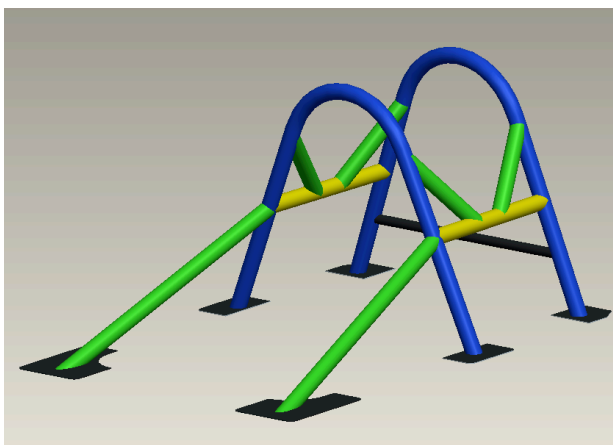


Figure 2.4: Roll Cage Components

The roll cage is composed of 5 main parts:

Front hoop (blue): The front hoop is located in front of the driver and extends from the top chassis panel to just above the driver's head. It will protect the driver by deflecting any moving bodies such as the shell or canopy during an impact. Directly beneath the front hoop is a bulkhead that acts as a lift-point on the car as well as a rigid support for the roll cage.

Rear hoop (blue): The rear hoop is located 12.5 [in.] behind the front hoop at the back of the driver compartment opening. The attachment point to the chassis is located directly above the vertical chassis panels running the length of the car to ensure that this point is rigid.

Forward slanting braces (green): The purpose of the forward slanting braces is to cover the driver's hands and steering wheel and also to give strength to the structure when force is applied in the fore-aft direction. The forward most point of this roll cage component attaches to the chassis directly above the vertical chassis panels running the length of the car.

Horizontal center braces (yellow): The horizontal center braces were placed just below the driver's sightline. They connect the front and rear hoops and act to stabilize the structure while taking some of the load in an impact.

Center cross braces (green): The center cross braces act to decrease the large moment created in an impact due to the yellow horizontal braces being placed below the driver's sightline.

The roll cage is constructed from 1.250 [in.] outer diameter 4130 steel tubing of three different wall thicknesses. Shown in Figure 2.4, the green colored tubing represents a wall thickness of 0.035 [in.], the yellow colored tubing a wall thickness of 0.049 [in.] and the blue colored tubing a wall thickness of 0.083 [in.]. The tubing has a yield strength of approximately of 75,000 [psi]. The mounting brackets that attach the roll cage to the chassis top panel are made from 0.0625 [in.] 4130 steel sheet stock. All roll cage components were welded by professionals using the TIG welding process.

3 - Impact Analysis

3.1 - Total Mass and Center of Gravity

Coordinate	Reference	Weight Distribution	
		Front	Rear
X	Centerline	63.5%	36.5%
Y	Ground		
Z	Forward of Front Axle		
Component	Mass (lbm)	Y (in.)	Z (in.)
Chassis Panels	29.8	22.0	-45.0
Shell	93.0	19.0	-30.0
Batteries	71.0	15.0	36.5
Front Suspension	30.0	17.0	0.0
Rear Suspension	67.0	19.0	-88.7
Steering	5.0	24.0	0.0
Brakes	7.0	24.0	0.0
Roll Cage	14.8	27.0	-68.3
Driver	176.0	18.0	-58.1
EE	22.0	12.0	24.0
Array	46.5	23.0	-33.5
Total	562.1	17.7	-32.8

The distance between the center of gravity of the vehicle and the centerline of the car (x-plane) can be neglected since all of the components with dominant mass have a center of gravity on the centerline of the car. Some smaller miscellaneous components of the car were not included in the table above and therefore the car with driver is estimated as 600 [lbs] for stress and force calculations. The longitudinal and vertical placement of the center of gravity contributes to the tip over stability of the vehicle. At 17.7 inches from the ground, the car will skid in a severe cornering maneuver well before it will tip over.

3.2 - Front Impact

In the event of a frontal collision, the nose of the shell would be crushed first followed by the battery and front of the chassis. There is then approximately 34 [in.] of chassis that would need to be crushed before the impacting body reached the driver's feet. The chassis and bulkheads at the front of the car extend from 12 [in.] to 23.3 [in.] above the ground plane; this easily accommodates the bumper height range given in the race regulations of 13.8 [in.] to 17.7 [in.]. Thus, in the event of a collision, the bumper of an impacting vehicle would transfer its forces directly to the structural chassis and bulkheads of the car. If the latches attaching the shell to the chassis were to fail causing the shell and array or the canopy to be pushed towards the rear of the car, the driver would be protected by the front supports and front hoop of the roll cage. These roll cage components would cause the top shell to deflect up and over the driver, leaving the driver compartment unobstructed.

The two vertical panels running the length of the car will take the majority of the force from an impact. This is a conservative estimate because in reality, a portion of the force would be distributed through the top and bottom panel of the chassis that connect the two vertical panels. The following calculations were done using the conservative estimate of only the vertical panels taking the load.

In a frontal impact, the two main modes of failure would be buckling or stress due to compression. Only one of the vertical panels and not the entire box beam structure is considered with the following buckling calculation and therefore the result is a vast underestimate of the total force required to cause the chassis to fail in buckling due to a 5G frontal impact.

The following equation for critical buckling force was obtained from *Successful Composite Techniques*, by K. Noakes, where d is the distance between median planes of the fiberglass skin, b is the height of the panel, E is the elastic modulus and K is the empirical buckling stress coefficient. The value for K was obtained from *Composite Materials: Design and Applications, Second Edition*, by D. Gay.

$$f_b = \left(\frac{d}{b}\right)^2 EK = \left(\frac{0.49in}{10.3in}\right)^2 (4.25E6psi)(1.0) = 9618.5lbs$$

The critical buckling force as calculated above is 9618 [lbs], which is 3.2 times the total force of 3000 [lbs] applied during a 5G frontal impact.

To find the stress due to compression in the panels from a 5G front impact, the equation $\sigma = F/A$ was used. Where area is the area of the fiberglass skin on the two vertical panels running the length of the car; $A = 4*10.3in*0.01in = 0.412 in^2$. The compressive stress produced in the panels was calculated to be $\sigma = F/A = (5*600lbs)/0.412in^2 = 7281.5$ [psi]. This yields a safety factor of 4.5 with respect to the critical stress of the fiberglass skins.

With a safety factor of 3.2 for failure due to buckling and a safety factor of 4.5 for failure due to compressive stresses, it can be concluded that the chassis can easily withstand a 5G front impact.

3.3 - Rear Impact

The height of the trailing edge of the vehicle's shell is 16 [in.], which is between the bumper height of 13.8 [in.] and 17.7 [in.] given by the regulations. This ensures that the trailing edge of the shell and array would be the first to be crushed upon a rear impact. The impacting body would then reach the rear suspension and the back of the chassis having a height ranging from 12 [in.] to 23.3 [in.], and finally the rear roll cage hoop. The crush space from the trailing edge of the car to the rear hoop of the roll cage totals 60 [in.].

In the event of a rear impact, the two modes of failure for the chassis would be the same as with a front impact, buckling or stress due to compression. Because the geometry of the chassis is the same in the front of the car as in the rear, the values for critical buckling

force and stress due to compression would be the same as described in the front impact portion. Since it was proven that the chassis could withstand a 5G front impact, it can therefore be assumed that the chassis could safely withstand a 5G impact from the rear.

3.4 - Bending Rigidity Under Vertical Loading

If we assume that the weight of the car is concentrated at the center of gravity, this produces a maximum moment of $M = F_F \cdot L_{CG}$, where F_F is the portion of the total weight of the car supported by the front suspension and L_{CG} is the distance from the front suspension to the center of gravity of the car.

$$M = F_F L_{CG} = [(Wt_{total} - Wt_{FS} - Wt_{RS}) \times 0.635] \times 32.8in = 10,476in \cdot lbs$$

$$\sigma = \frac{My}{I} = \frac{10,476in \cdot lbs \times 7.467in}{26.65in^4} = 2,935.4psi$$

The value for y and I were calculated based upon the area of the chassis that had the lowest moment of inertia – the front of the driver compartment where the top chassis panel is cut out. Also, these values were calculated just accounting for the skin of the composite panels as having inertia.

According to the calculations above, under static loading conditions the chassis has a safety factor of 11.2 with respect to failure. In the case of a roll over or a large bump (5G loading), there is a safety factor of just over 2.2.

3.5 - Side Impact

The driver resides in the center 22 [in] of the total 70 [in] wide car leaving 24 [in] of crush space on either side of the driver compartment in the event of a side impact. If the impact were to cause the array and/or canopy to come unattached, the front and rear roll cage hoops as well as the horizontal center supports would protect the driver's head and upper body from being harmed. These roll cage components would cause the impacting body to slide up and over the driver compartment.

A side impact near the center of the side of the car will be considered because such an impact would create the largest bending moment and therefore the largest stresses in the chassis.

The side impact can be treated similarly to the vertical loading scenario, just with a different moment of inertia with the 5G force acting horizontally instead of vertically on the chassis. Since there is a structural chassis panel stretching across the chassis near both the front and rear axle, both are treated as rigid supports with a 5G load applied at 32.4 [in.] from the front axle.

$$M = 5 \times F_F L_{CG} = 52,380in \cdot lbs$$

$$\sigma = \frac{My}{I} = \frac{52,380in \cdot lbs \times 17.25in}{174.9in^4} = 5166.1psi$$

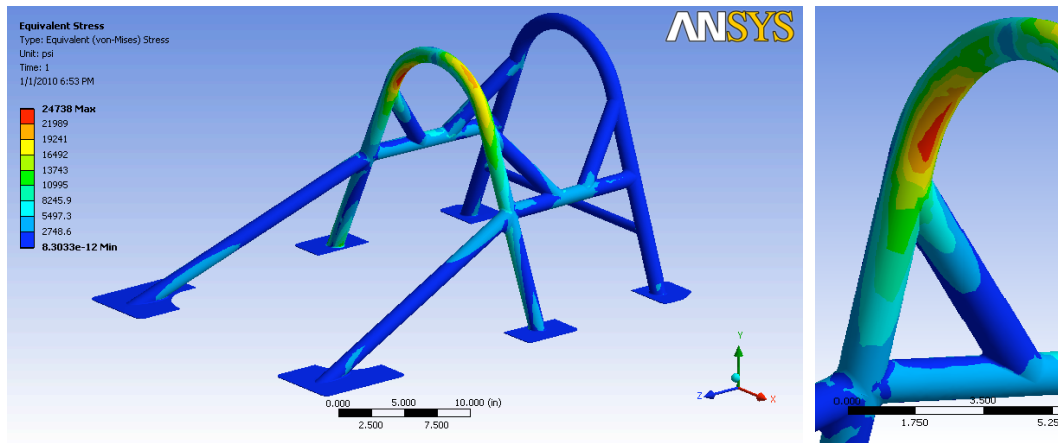
A maximum stress of 5,166.1 [psi] yields a safety factor of nearly 6.4 with respect to failure due to a 5G side impact.

3.6 - Rollover Analysis

In a rollover situation the roll cage and chassis would support the vehicle. Any loads applied to the roll cage would be transferred to the chassis in such a situation. Since it has already been proven that the chassis can withstand greater than 4G loading, the roll cage attachment points to the chassis are treated as rigid in the following analysis.

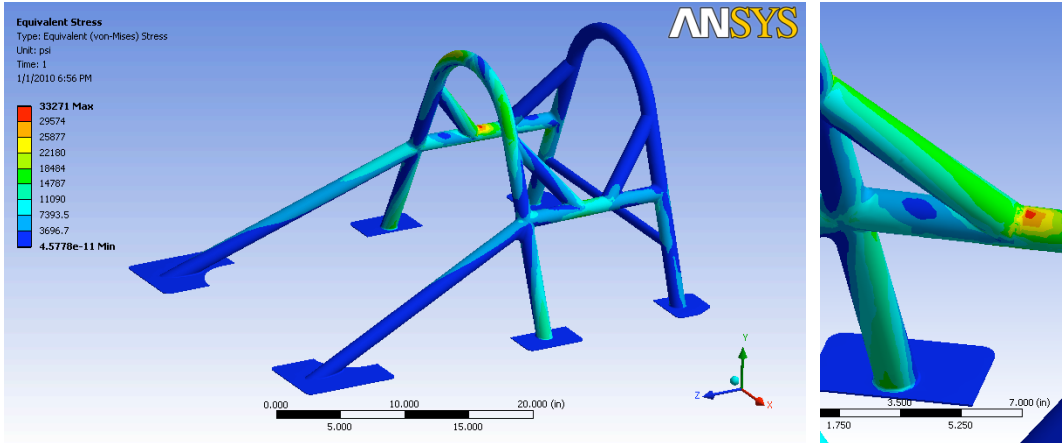
Roll cage simulations were done using finite element analysis. The software package used was ANSYS Workbench version 11. All simulations done were static structural using tetrahedral elements with a relevance factor of 60. All loads were applied solely to the front hoop of the roll cage as a worst case scenario situation. During most rollover situations, the load would be shared by either the front of the chassis and the front hoop or both the front and rear hoop. With the possibility of the front hoop taking the entire load, this was treated as the loading situation. Stresses were calculated using the equivalent (von-Mises) stress model. A vehicle weight of 600 [lbs] was used in all of the roll cage simulations. All of the simulations to follow include an isometric view of the equivalent stress result as well as a close-up image of the area of highest stress.

3.7 - 4G Vertical Load



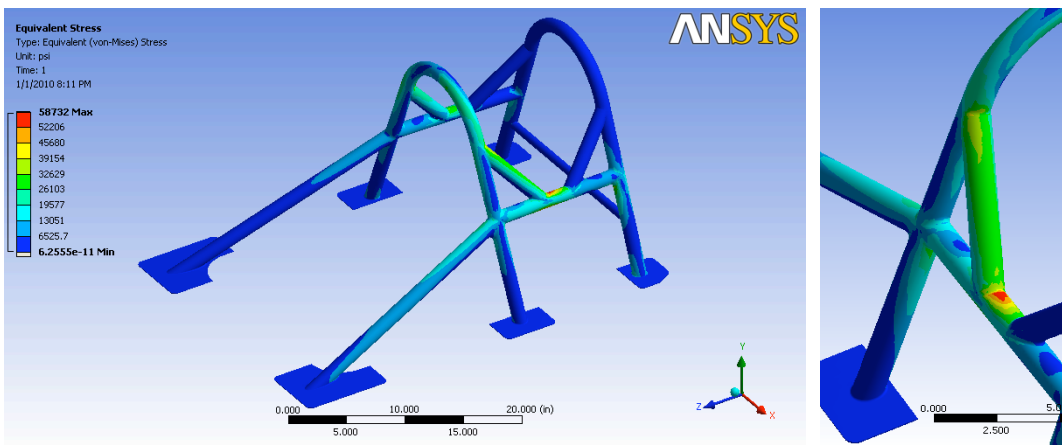
For this loading condition, the highest stresses were found near where the center cross braces attach to the front hoop. Since this is where the largest bending moment is occurring, it seems logical that the maximum stress would be found here. The highest stress seen was 24,738 [psi], leaving a safety factor of just over 3 with respect to the yield strength of 4130 steel, which is 75,000 [psi].

3.8 - 4G Load, 22.5° Forward from Vertical



The highest stresses for this loading scenario were found where the center cross braces attach to the horizontal center braces. Since the front and rear hoops are constructed from larger wall thickness tubing than the horizontal braces, it seems logical that the highest stress would be found at this intersection and not where the center cross braces attach to the front hoop. These two places are where the bending moment induced by the 4G loading was the highest. The highest stress found was 46,066 [psi]. This value is in between the values of maximum stress found for the vertical loading and the forward 45° loading scenarios, which is intuitive since the 22.5° angle that the load was applied at is between the 0° and 45° load. The maximum stress in this loading condition yields a safety factor of 2.3.

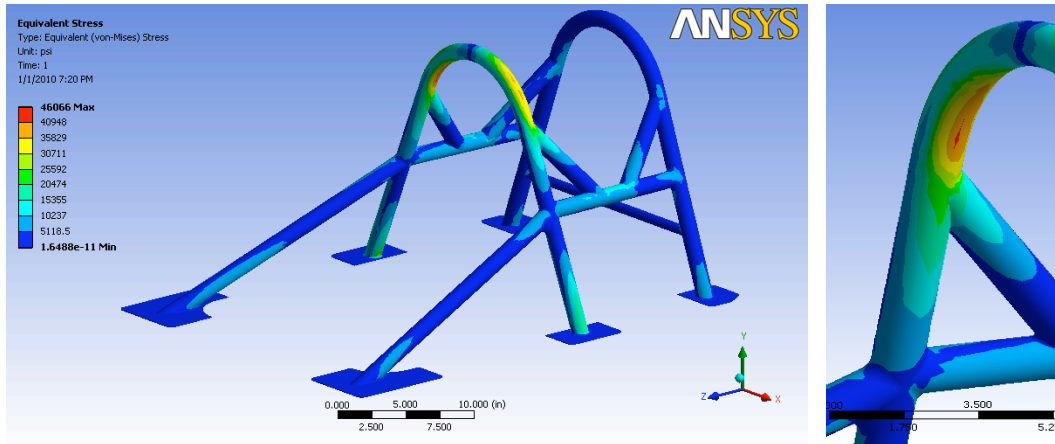
3.9 - 4G Load, 45° Forward from Vertical



As can be seen in the above-right image, the highest stresses for the 45° from vertical loading scenario were found around where the center cross brace attaches to the horizontal brace. This is the same place that the highest stress was found with the 22.5° forward loading condition. With this kind of geometry, the maximum stress should be found in the same general area for these two loading conditions. The larger rearward

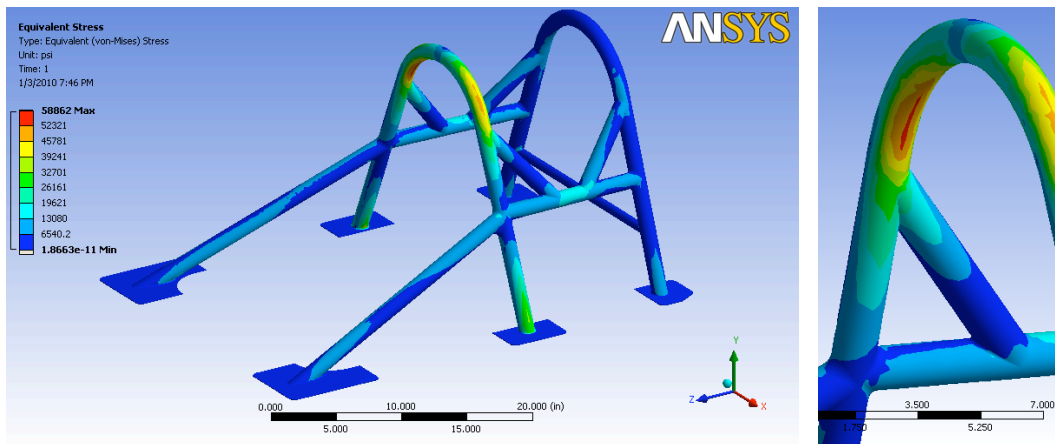
component of the impact force causes the stress in this situation to be greater than in the 22.5° situation. The maximum stress found was 58,732 [psi], which leaves a safety factor of 1.3 with respect to yielding.

3.10 - 4G Load, 22.5° Lateral from Vertical



The maximum stress found in this loading scenario was 46,066 [psi], which yields a safety factor of just over 1.6. This value seems logical since a force applied at 22.5° should produce a stress somewhere in between the stress produced from a force at 0° and 45° from lateral.

3.11 - 4G Load, 45° Lateral from Vertical



The areas of maximum stress for this loading condition were the area near where the front hoop and center cross braces attach as well as the area where the front hoop attaches to the chassis. These two areas are where the largest bending moments are created due to the 45° lateral force. The maximum stress created was 58,862 [psi]. This leaves a safety factor of 1.3 with respect to yielding of the roll cage in a rollover situation.

3.12 - Battery Enclosure

The battery box is made using the same construction as the chassis. The box is removable and attached to the chassis side panels via four grommets. Loading these four grommets in shear supports the weight of the box. There is a horizontal panel directly below the battery box that is tabbed into the side panels of the chassis to add torsional strength to the system as well as to aid in supporting the box. Between the battery and the driver compartment are the back panel of the battery box, the power tracker boxes, and the front panel of the chassis. Therefore, at least 4 panels would need to be penetrated before any of the batteries were to contact the driver.

The cells are secured inside the box using 3M™ Hi-Strength 90 Spray Adhesive. This system has been proven on Borealis III and Centaurus I, and provides a measure of vibration resistance for the fragile electrical connections between cells. Battery cooling is accomplished through the use of eight 60 [mm] fans. The air is then vented out of both the left and right wheel well.

4 - Brakes

4.1 – System Specifications

Centaurus II uses two independent hydraulic braking systems. The mechanical braking is assisted by regenerative braking through the motor at the rear wheel.

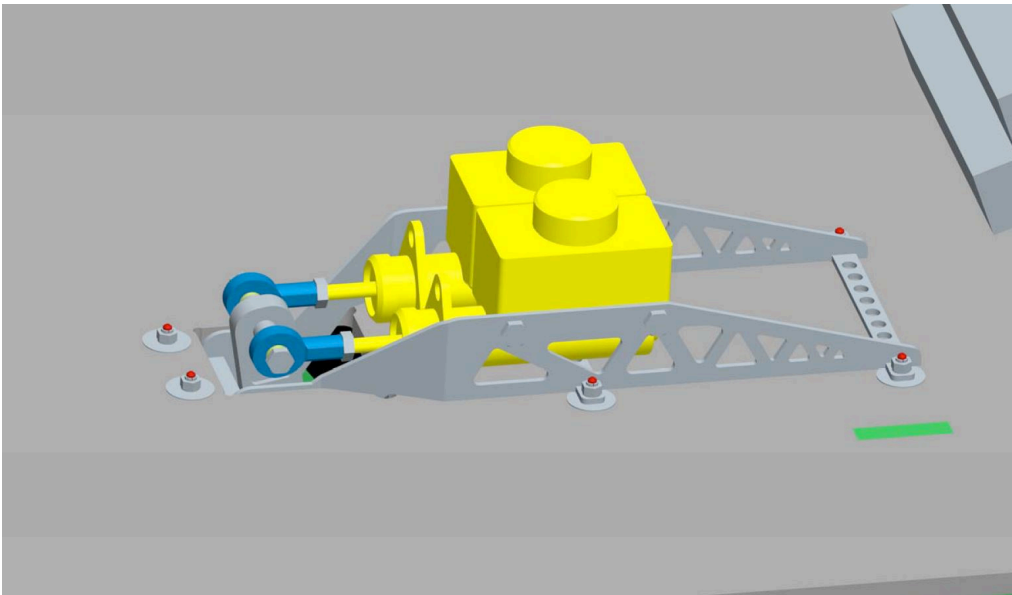


Figure 4.1: The master cylinder and pedal assembly as viewed from above the chassis

Each hydraulic system has a master cylinder with a 0.75 [in] diameter piston which actuates a caliper cylinder at each front wheel. The master cylinders are supplied from CNC, Inc, and are made out of aluminum with steel sleeves. The calipers are supplied

from Martin Custom Products and have 1.00 [in] diameter pistons. There is a custom 8.000 [in] diameter brake disc at each of the front wheels. The discs will be machined from 7075-T6 Aluminum and Alpha coated by Surface Solutions in Fridley, MN. Alpha coating produces a hard, wear resistant surface. A custom pedal assembly actuates both hydraulic systems simultaneously and is adjustable to balance wear on the pads. The regenerative brake is controlled with a lever on the steering wheel. Lock-nuts are used on bolts where there are no turning parts and castle nuts with either cotter pins or safety wire are used on the bolts fastened to rotating parts.

4.2 - Loading Conditions/System Analysis

The braking system is designed to be limited only by friction between the tires and the road. A pedal force of 100 [lbf] will supply line pressure of 176.8 [psi] and produce deceleration of 0.50 [G]. The master cylinders are rated for 1200 [psi]. If one hydraulic system fails, there will still be a working caliper on each wheel and the pressure in the remaining system at 100 [lbf] of driver input force would double to 353.6 [psi] which is still below the rated value. The pedal will be constructed from 0.5 [in] x 1.25 [in] 7075-T6 aluminum, and machined into a modified I-beam design. The maximum bending stress of the pedal under double the required force (200[lbf]) results in a safety factor of 1.81.

The master cylinder and pedal assembly will be mounted on top of the chassis where the pedal enters into the driver compartment from the top as shown in Figure 4.1. The assembly is mounted to the chassis using six 5319 SERA aluminum inserts as described in section 2.2. A pedal force of 200 [lb] results in a 705.6 [lb] reaction loading the six bolts and grommets in shear on each bracket. There is also a moment produced that loads the six grommets well below their tested strength. The main master cylinder bracket will be water jet cut from 6061-T6 Aluminum, and bent to the shape shown in Figure 4.1.

5 – Front Suspension

5.1 - Materials and Layout

The front suspension is arranged in a double a-arm layout designed to minimize tire scrub and weight. The lower a-arms are made of 0.750 [in] OD by 0.058 [in] wall thickness 4130 steel tubing. The upper a-arms are machined into a 0.5 [in] by 0.5 [in] section from 7075-T6 Aluminum. Both sets of a-arms use Aurora Bearing rod ends (HXAM-4T) on the chassis side and Aurora spherical bearings (HAB-4T) on the upright side. The brackets for both sets are made from 6061-T6 aluminum. The front suspension uses Army/Navy or military spec nuts, bolts and washers. All structural brackets are secured to the chassis with at least 3 bolts and 5319 SERA aluminum inserts (section 2.2).

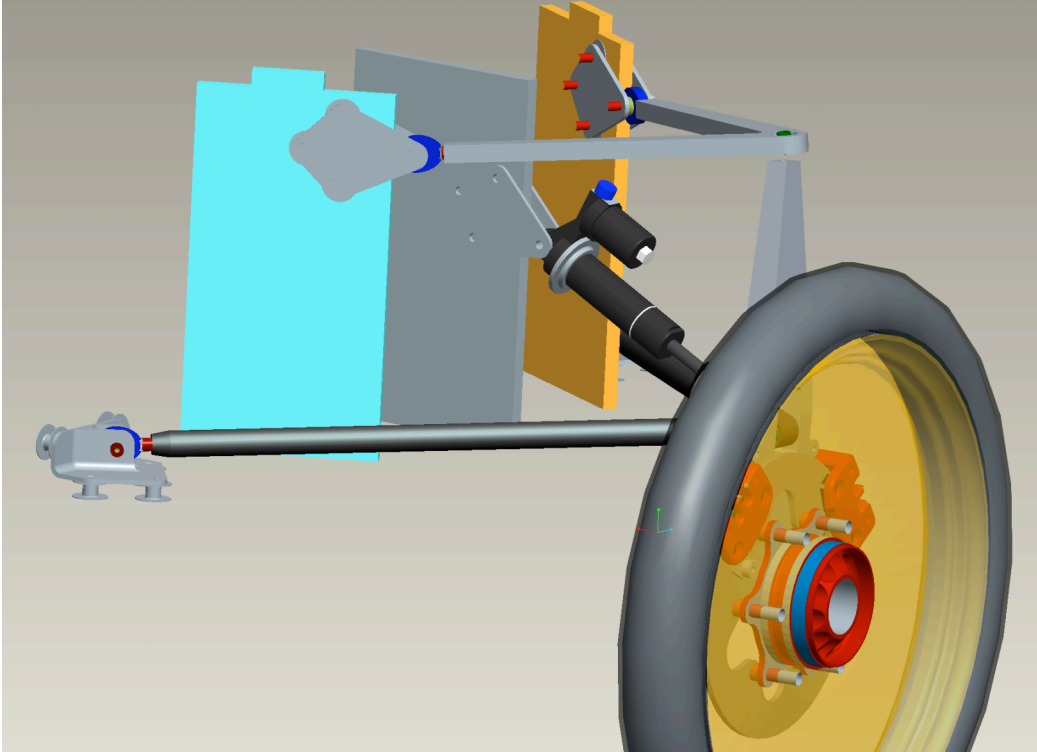


Figure 5.1: CAD Image of Front Suspension, Steering Not Shown

5.2 - Wheels, Tires, Hubs, and Axles

We will be using NGM wheels with Bridgestone Ecopia EP-80 tires. From section 3.1, the weight carried by the front wheels is 178 [lb] each, and by the rear wheel is 205 [lb]. These weights are well within the load rating of the tires. The left side hub uses a LH threaded nut, and the right side hub uses a RH threaded nut to ensure retention. All hub nuts utilize safety wire to prevent loosening. All components in this section are identical to those used by the UMNSVP on our past 2 vehicles raced in NASC without incidence with a near identical car weight.

See Appendix (A5) for force calculations used in the following stress analyses

5.3 - A-Arm Buckling Analysis

A buckling analysis of the upper and lower A-arms gives the following critical loads. For a more detailed description of the analysis used, please refer to http://www.engineersedge.com/column_buckling/column_ideal.htm

Upper A-arm Critical Numbers

Width, $W = 0.50$ [in.] (at minimum)

Height, $H = 0.50$ [in.]

Length, $L = 10.23$ [in.]

Material = 7075 T-6 Aluminum

$E = 1.04E+7$ psi

Yield Stress, $\sigma_y = 67E+3$ psi

Calculations

$$\text{Moment of Inertia, } I = \frac{W * H^3}{12} = .005208 \text{ in}^4$$

$$\text{Cross Sectional Area, } A = W * H = .25 \text{ in}^2$$

$$\text{Radius of Gyration, } r = \sqrt{\frac{I}{A}} = .144 \text{ in}$$

$$\text{Slenderness Ratio, } S = \frac{L_e}{r} = 70.9$$

$$\text{Critical Slenderness Ratio, } S_{cr} = \sqrt{\frac{2\pi^2 E}{\sigma_y}} = 54.3$$

Therefore, we use Johnson's Equation for a short beam.

$$\text{Critical Load, } P_{cr} = \sigma_y A \left(1 - \left(\frac{\sigma_y}{4\pi^2 E} \right) \left(\frac{L_e}{r} \right)^2 \right) = 1430 \text{ [lbf]}$$

Calculated Worst Case Compressive Load = 480 [lbf]

Safety Factor = 2.98

Lower A-arm Critical Numbers

Outer Diameter, OD = 0.75 [in.]

Thickness, t = 0.058 [in.]

Length, L = 18.29 [in.]

Material = 4130 Steel

E = 3.00E+7 Psi

Yield Stress = 75E+3 Psi

Calculations

$$\text{Moment of Inertia, } I = \frac{\pi}{4} \left(\left(\frac{OD}{2} \right)^4 - \left(\frac{OD-t}{2} \right)^4 \right) = .004275 \text{ in}^4$$

$$\text{Cross Sectional Area, } A = \pi \left(\left(\frac{OD}{2} \right)^2 - \left(\frac{OD-t}{2} \right)^2 \right) = .06568 \text{ in}^2$$

$$\text{Radius of Gyration, } r = \sqrt{\frac{I}{A}} = .2551 \text{ in}$$

$$\text{Slenderness Ratio, } S = \frac{L_e}{r} = 71.7$$

$$\text{Critical Slenderness Ratio, } S_{cr} = \sqrt{\frac{2\pi^2 E}{\sigma_y}} = 71.7$$

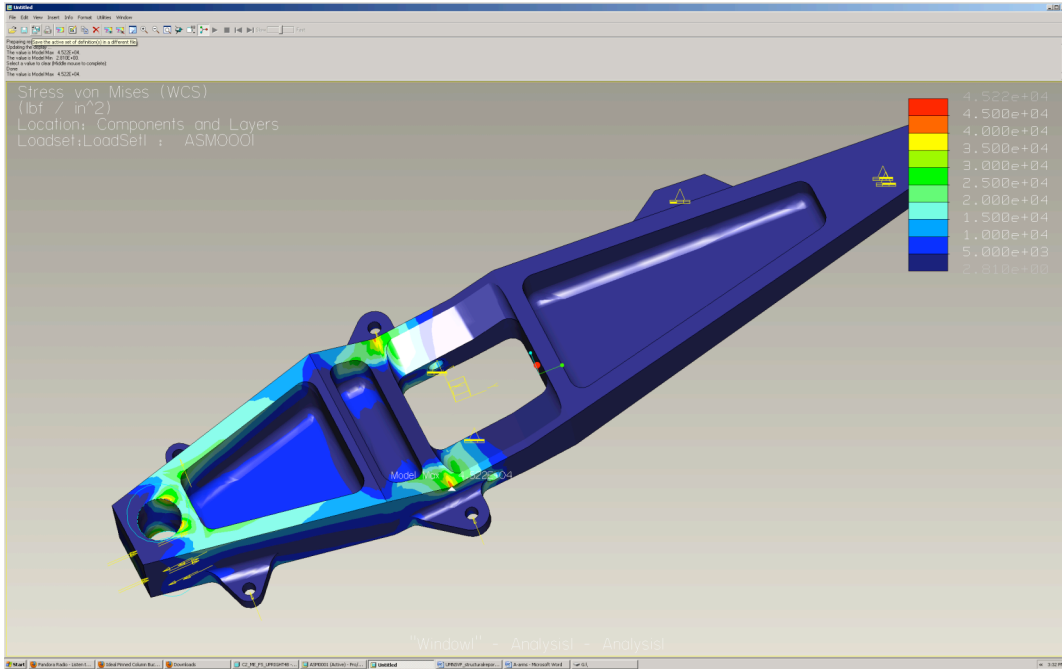
$$\text{Critical Load, } P_{cr} = \sigma_y A \left(1 - \left(\frac{\sigma_y}{4\pi^2 E} \right) \left(\frac{L_e}{r} \right)^2 \right) = 3320 \text{ [lbf]}$$

Calculated Worst Case Compressive Load = 1426 [lbf]

Safety Factor = 2.33

5.4 - Upright Stress Analysis

The stress analysis for the upright was done with Pro/Engineer Mechanical, a brand of finite element analysis. The upright is made from 7075-T6 Aluminum with a yield stress of 73 [ksi]. The results when loaded with the calculated forces (section A5) are shown in the figure below.



The maximum von Mises stress is 45 [ksi] giving a safety factor of 1.622 under simultaneous 4G bump, 1G braking and 1G cornering.

6 – Rear Suspension

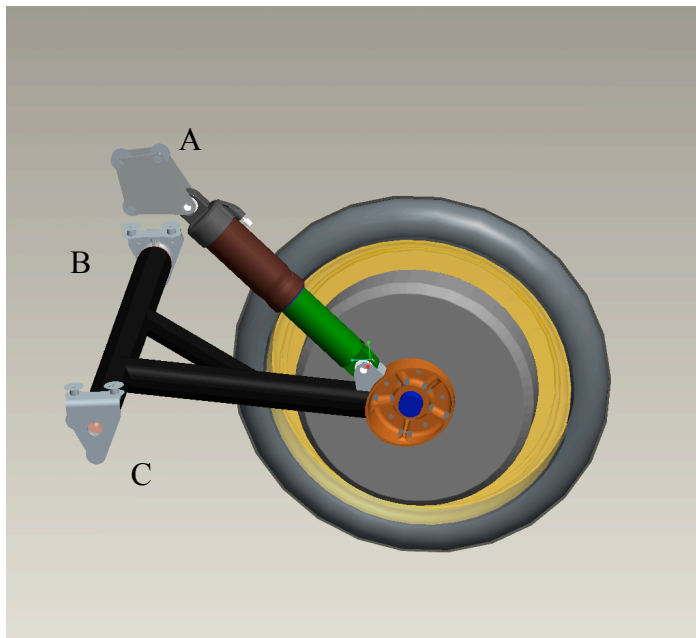


Figure 6.1: CAD Image of Rear Suspension

6.1 – Materials Specifications

The rear suspension system utilizes a swing arm design similar to that used for the previous car. The swing arm is made of 1.75 [in.] OD by 0.083 [in.] wall thickness 4130 steel tubing with a 1.25 [in.] OD bracing arm and motor mount milled out of 4130 steel. The swing arm tubes and motor mount are professionally welded using the TIG process into the layout illustrated in Figure 6.1, where the swing arm is in black, and the motor mount in orange.

The swing arm is attached to the chassis through brackets machined out of 7075-T6 Aluminum. Each bracket contains bearings and is attached to the chassis using five 5319 SERA aluminum grommets (section 2.2). Each grommet can handle 1500 [lbs] of shear load, so that the combined grommets of each bracket can easily support the maximum loads applied at the mounting points of the swing arm.

The swing arm is also connected to the chassis via a Fox Float RC shock, mounted to the swing arm with a bracket machined out of 4130 steel, and to the chassis with two brackets made from 6061-T6 aluminum.

6.2 – System Analysis

See Appendix for force calculations (A6.1) and stress analysis (A6.2-6.3).

6.3 – Parking Brake

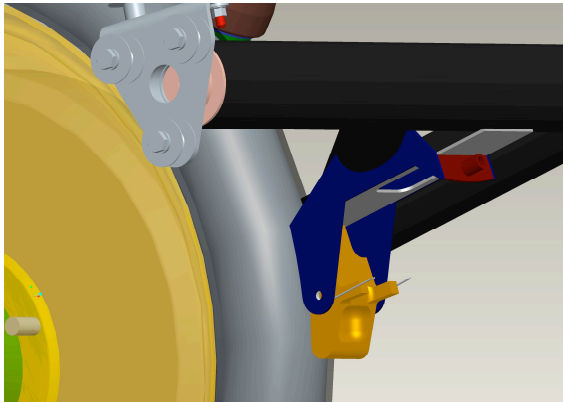


Figure 6.2: CAD Image of Parking Brake

The parking brake acts at the rear tire. It is mounted to the swing arm as shown in Figure 6.2 and will be actuated via a lever near the side of the driver compartment. Calculations will be done to show that the car will not slide down a 10% incline if the parking brake is engaged.

7 – Steering

7.1 - Material Specifications

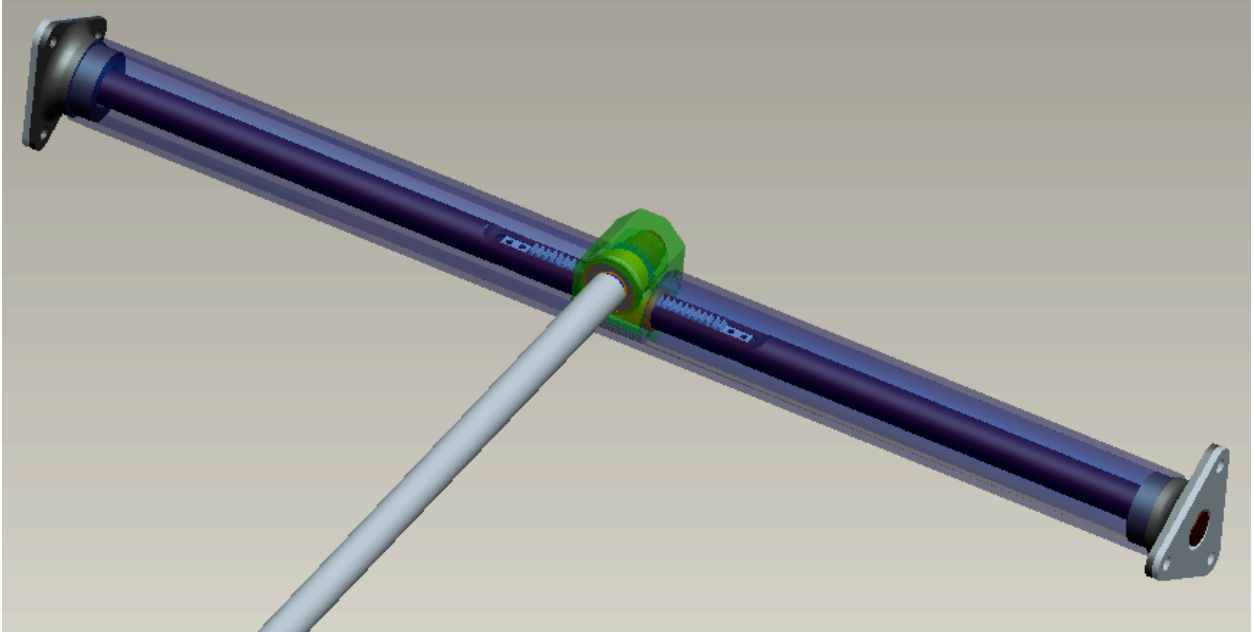


Figure 7.1: Gear Box with custom rack, rack cover, and chassis attachment brackets

A rack and pinion system will be employed to steer the vehicle. A composite steering wheel will be coupled to a steel drive shaft. The drive shaft is coupled to a steel pinion gear. The pinion gear mates with a steel rack attached to an aluminum shaft inside a custom machined aluminum gear box. The aluminum shaft is made of a 6061 T-6 aluminum of diameter 0.625 [in]. The purchased steel rack rests in a milled groove as shown in Figure 7.1 and is secured with two rivets on each end. The pinion inserts into the gear box and is held in place by a snap ring.

Rack motion is transmitted to the front suspension uprights through aluminum tie rods with Aurora Bearing rod ends (HXAM-4T). The main tie rod shaft keeps its orientation with the pinion gear through its orientation with bushings that contact the flat portion of the rack. Bushings are to be constructed of either bronze or nylon. All fastening hardware is aircraft grade AN or NAS series bolts and fasteners.

The use of a rack and pinion has been successfully used in many steering systems in a variety of vehicle designs. The steering system also employs near perfect Ackermann geometry, and minimal bump steering well within the physical limits of the suspension. Since the driver is situated far behind the front wheels, there is room to design a steering system with acceptable Ackermann angles. This design leads to minimal tire scrub during cornering and minimal tire wear. The steering angles were calculated for both an 11 and 8 meter turn radius. The maximum turn angle was found to be 21.1° on the inside wheel of an 8 meter turn.

7.3 – System Analysis

To trace loads from the ground up to the tie rods, we use the situation of a 1G turn and a 1G brake load as the ‘worst case’ scenario. With a 5° castor, and a 5° camber, we have a calculated Scrub Radius of 0.556 [in], and a Mechanical Trail of 0.81 [in]. Statics was then used to determine the force exerted on the tie rods. With an estimated vehicle weight of 614 [lbs], the maximum force on the tie rod shaft during this cornering situation is 111 [lbs] in compression. With a yield strength for this material of $S_y = 37$ [ksi], and an uncut area under compression of 0.15 [in²], $\sigma = \frac{111 [lb]}{0.15 [in^2]} = 738.4 [psi]$.

Therefore, yielding due to compression will not occur.

To determine whether the rack will buckle under a combined turning and braking force, we will use the equation for buckling with pinned ends: $P_{crit} = \frac{\pi^2 EI}{L^2}$. Where L = 22 [in.]

(The length of rod inside the chassis), E = 10000 [ksi] for 6061 T-6 Aluminum, and I is calculated using: $I = \frac{\pi r^4}{4}$. The uncut radius, r = 0.21875 [in], will be used. The critical

buckling force is then calculated to be:

$$P_{crit} = \frac{\pi^2 EI}{L^2} = \frac{\pi^2 \left(10000 \left[\frac{klb}{in^2} \right] \right) \left(\frac{\pi (0.21875 [in])^4}{4} \right)}{(22 [in])^2} = 366.7 [lb]$$

This is greater than the 111 [lb] maximum force exerted during a 1G turn and 1G brake scenario. Note that this is a conservative estimate because, in reality, there will be some distribution of the 111 [lb] force transmitted to the chassis by the rack cover. This calculation equates to a safety factor of 3.3.

Appendix

A2 – Chassis

A2.1 - Material Properties of Teklam N505-1 Fiberglass Paneling

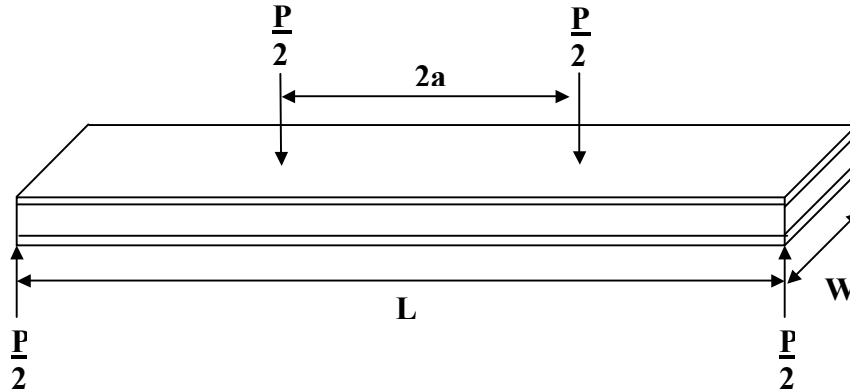


Figure A2.1: Four-point bending test setup.

Variables:

Skin Thickness $t = 0.01$ in.

Panel Thickness $h = 0.5$ in.

[Testing done at the University of Minnesota]

Total Length: $L = 6$ in.

Width: $W = 1$ in.

Distance Between Loads: $a = 5/6$ in

[Data from Teklam material specifications]

Total Length: $L = 20$ in.

Width: $W = 3$ in.

Load at Failure: $P_{crit} = 190$ lbs.

Distance Between Loads: $a = 5$ in.

Critical Stress:

The maximum moment can be calculated using data from the Teklam spec sheet and testing procedure document.

$$M_{max} = \left(\frac{P_{crit}}{2}\right) \times a = \left(\frac{190lb}{2}\right) \times 5in = 475in \cdot lbs$$

$$I_x = I_{0.5} - I_{0.48} = \left[(1/12)(3in)(0.5)^3 - (1/12)(3in)(0.48)^3 \right] = 0.0036in^4$$

$$\sigma_{crit} = \left(\frac{-M_{max}y}{I_x}\right) = \left(\frac{475in \cdot lbs \times 0.25in}{0.0036in^4}\right) = 32,986psi$$

Elastic Modulus:

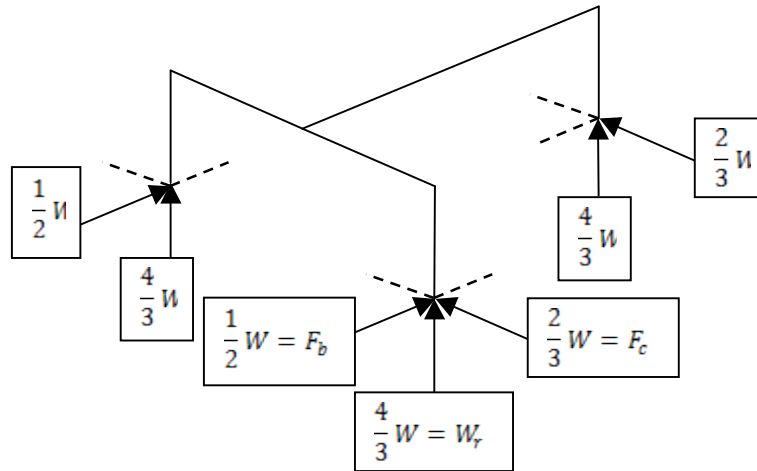
The Elastic Modulus was determined from four-point bending tests done using equipment from the Aerospace Engineering department at the University of Minnesota. Test setup data is shown above. Four sample Teklam N505-1 specimens were tested and their respective Elastic Modulus values were averaged giving the following value:

$$E = 4.25E6psi$$

A5 – Front Suspension Force Calculations

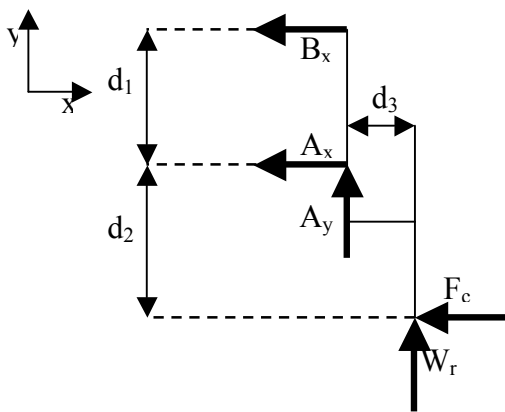
A5.1 - Force Calculations

In order to determine loading conditions for the front suspension, top, right and front view free body diagrams were drawn for the upright and A-Arms. By using the fact that the sum of forces and moments on the suspension are equal to zero, reaction forces to braking, cornering and bump input forces were calculated. The worst case loading condition used for the calculations was a 1G braking force, 1G cornering force and 4G bump force. Since the solar car will only have three wheels, the distribution of vehicle weight under these conditions follows the diagram below. W , F_c , W_r and F_b are vehicle weight, cornering force, bump force and braking force, respectively. Only the front wheels perform braking.

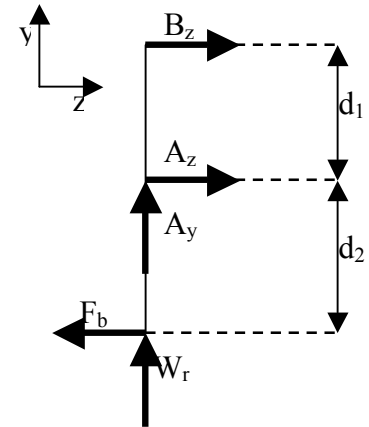


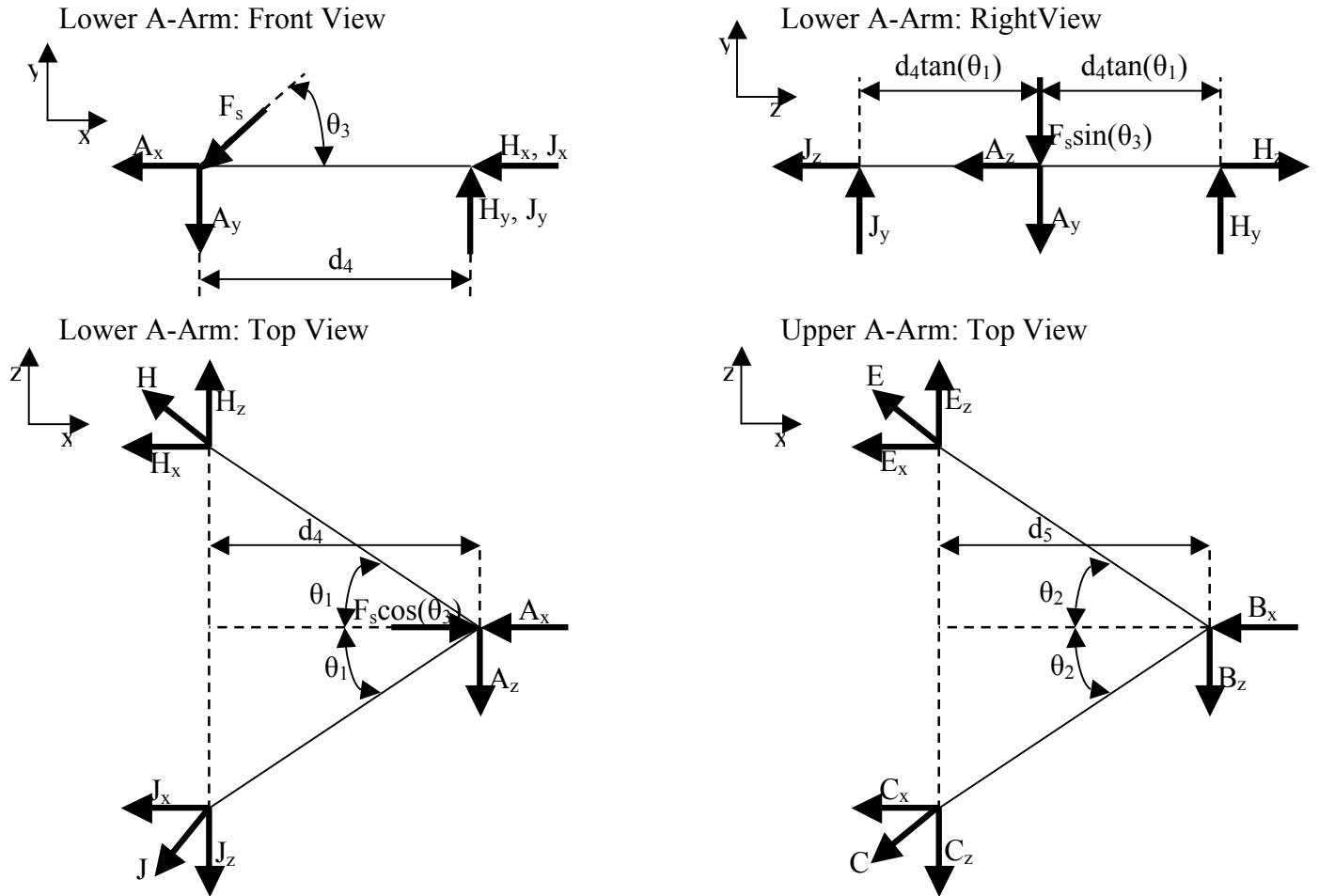
The forces in the diagram above were used to create the free body diagrams, and force equations were solved for in terms of these forces. The free body diagrams used are shown below. A_x , A_y , A_z , B_x , B_z , C , C_x , C_z , E , E_x , E_z , H , H_x , H_y , H_z , J , J_x , J_y and J_z are reaction forces on the upright and A-Arms. F_s is the force from the shock absorber.

Upright: Front View



Upright: Right View





The equations calculated from the free body diagrams were compiled in an Excel spreadsheet so that the values of the reaction forces at maximum loading could be seen. Force equations were also calculated using Matlab code and Excel macros. By doing the analysis both by hand and in Matlab, we were able to double check the accuracy of the Matlab code. A sample table from the Excel sheet with hand calculations is shown below. The calculations were made by assuming that the weight of the car is 600 lbs. All distances are in inches, angles in both degrees and radians, and forces in lbs.

D1(in)	13.7844	Wr(y)	800
D2(in)	8	Fb(z)	300
D3(in)	1.75	Fc(x)	-400
D4(in)	14	Ax	1264.22
D5(in)	8.858	Ay	-800
θ1(rad)	0.698131	Az	816.915
θ2(rad)	0.523598	Bx	-864.22
θ3(rad)	1.047197	Bz	-516.915
(D1+D2)/D2	2.72305	C	1015.873
(D3/D2)	0.21875	Cx	879.772
		Cz	507.9361

$\theta 1(\text{deg})$	40	E	-17.9579
$\theta 2(\text{deg})$	30	Ex	-15.552
$\theta 3(\text{deg})$	60	Ez	-8.97893
		H	111.7583
		Hx	85.61186
		Hy	0
		Hz	71.83679
		J	-1159.14
		Jx	-887.951
		Jy	0
		Jz	-745.078
		Fshock	923.7609
		Fshock(x)	461.8812
		Fshock(y)	-800

A6 - Rear Suspension System Analysis

A6.1 - Rear Suspension Force Calculations

The rear wheel receives a worst case 4g bump load and a 1g cornering load. The braking and acceleration loads are so small as to be insignificant to this analysis.

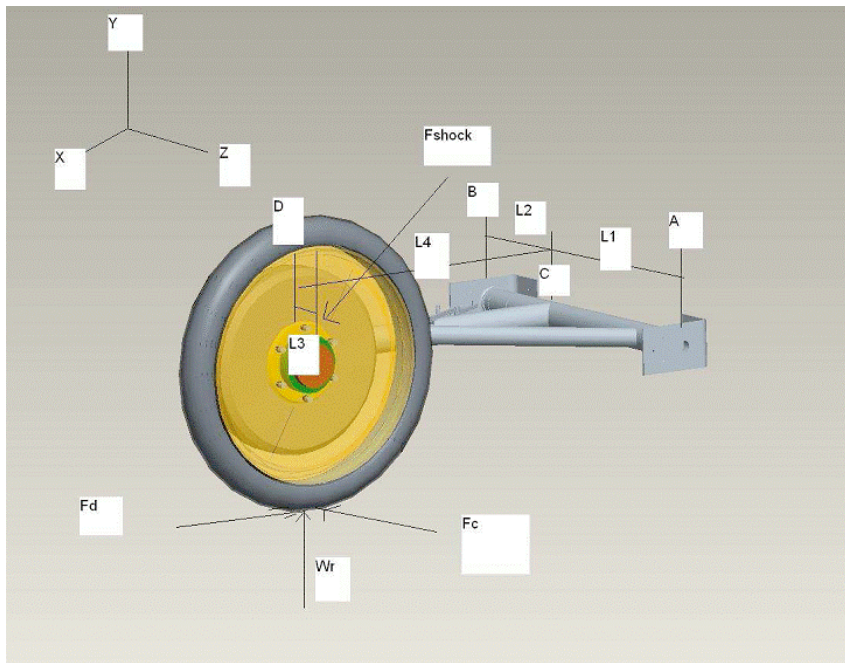


Figure A6.1a, CAD Image of Swing arm geometry

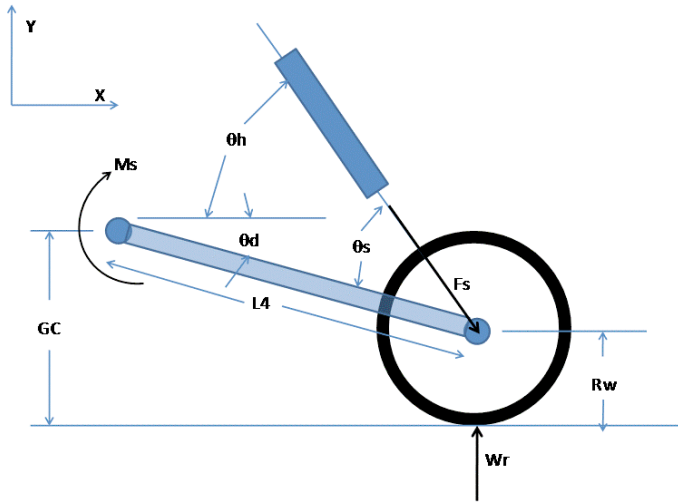


Figure A6.1b, Side View of Rear Swing Arm

$$\theta_d = \tan^{-1}\left(\frac{GC - R_w}{L4}\right)$$

The angle the shock makes with the swing arm is θ_s . The angle the shock makes with the horizontal is θ_h where:

$$\theta_h = \theta_s + \theta_d$$

The summation of the moments about the swing arm axis (M_s) is used to compute the shock force F_s as a function of the angles and the weight reaction force W_r .

$$\sum M_s = L4 \sin(\theta_s) F_s - W_r \cos(\theta_d) L4 = 0$$

$$F_s = \frac{W_r \cos(\theta_d)}{\sin(\theta_s)}$$

Now we can compute the horizontal (x component) and vertical (y component) of the shock force on the swing arm (and the shock mount bracket).

$$F_{sy} = F_s \sin(\theta_h)$$

$$F_{sx} = F_s \cos(\theta_h)$$

The top view of the swing arm is:

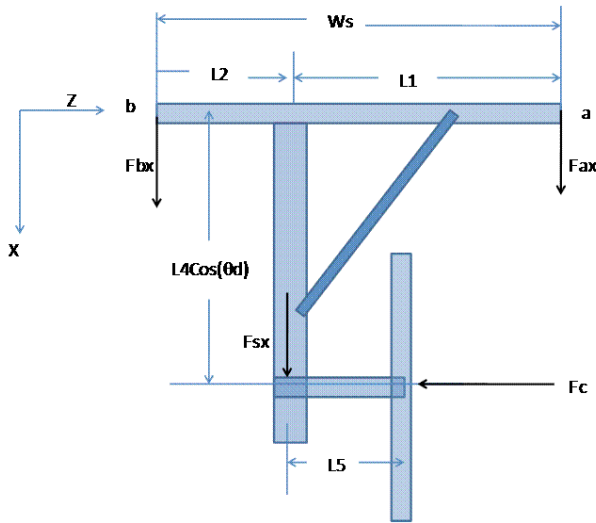


Figure A6.1c, Top View of Geometry

The swing arm length from the rotation axis to the rear axle along the arm is L4. It is foreshortened in this view by the angle it drops down (θ_d), so its horizontal (x axis) length is $L4\cos(\theta_d)$.

First we take the summation of the moments clockwise about point 'b' to get an equation for the unknown reaction force Fax.

$$\sum M_b = WsFax + FcL4 \cos(\theta_d) + FsxL2 = 0$$

$$Fsx = Fs \cos(\theta_h)$$

$$Fax = \frac{-FcL4 \cos(\theta_d) - Fs \cos(\theta_h)L2}{Ws}$$

Next we take the clockwise moments about the point A (driver's right side) to get an equation for the left side reaction force Fbx.

$$\sum M_a = -WsFbx + FcL4 \cos(\theta_d) - FsxL2$$

$$Fsx = Fs \cos(\theta_h)$$

$$Fbx = \frac{FcL4 \cos(\theta_d) - Fs \cos(\theta_h)L2}{Ws}$$

The sum of all the forces in the X direction must be zero. The sum of all forces in the X direction is $(Fbx+Fax +Fsx=0)$.

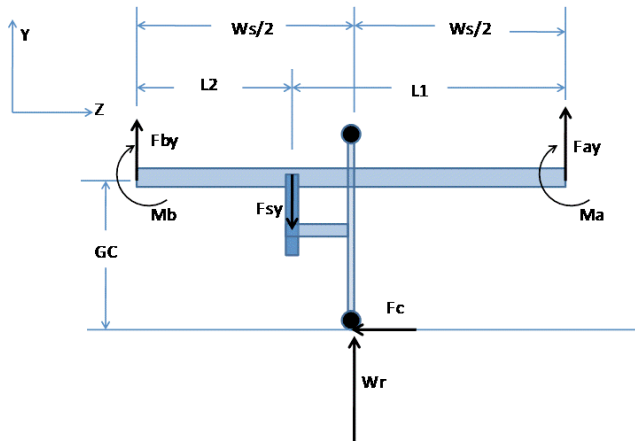


Figure A6.1d, Rear View of Swing Arm Geometry

As before we take the clockwise summation of moments about point 'b' then the other end point 'a' and solve for the reaction forces F_{by} and F_{ay} in terms of the geometry and the forces acting on the swing arm F_{sy} (vertical component of shock force), W_r , and F_c .

$$M_b = F_{sy} L_2 + F_c GC - W_r W_s^2 - F_{ay} W_s = 0$$

Solving for F_{ay} gives:

$$F_{ay} = \frac{F_{sy} L_2 + F_c GC - W_r W_s^2}{W_s}$$

Recall $F_{sy} = F_s \sin(\theta_h)$ substitute that in above to complete the derivation for F_{ay} .

$$F_{ay} = \frac{F_s \sin(\theta_h) L_2 + F_c GC - W_r W_s^2}{W_s}$$

The same process for the moment about the right hand side M_a gives an equation for F_{by} .

$$M_a = -F_{sy} L_1 + F_c GC + W_r W_s^2 + F_{by} W_s = 0$$

Now we solve for F_{by} and substitute F_{sy} as before.

$$F_{by} = \frac{F_s \sin(\theta_h) L_1 - F_c GC - W_r W_s^2}{W_s}$$

Twisting moment about swing arm tube

$$M_t = F_c R_w - W_r L_5 \cos(\theta_d)$$

A6.2 - Resulting Force Spreadsheet

forces			car weight
braking	200		600
cornering	200		
bump	800		

cases	bump	cornering right		bump + turn right		bump + turn left		Safety Factor
Reaction Forces								
Shock bracket A	1131.3708	0		1131.37		1131.3708		3.97747564
Reaction C vertical	155.93925	90.573665		65.3656		246.51291		18.2546218
Reaction C Horizontal	564.81356	240.629891	worst case	419.704	worst case	224.22975	worst case	5.3114872
Reaction B vertical	-155.93925	-90.573665		-65.3656		-246.5129		18.2546218
Reaction B Horizontal	235.18644	240.629891	worst case	475.154	worst case	726.67909	worst case	4.12836979

cases	bump		cornering right		bump + turn right		bump + turn left	
	arm	swing beam	arm	swing beam	arm	swing beam	arm	swing beam
normal	1851.0593	19008.245	16309.7	11240.49	17109.716	8167.75053	17109.716	29848.7395
shear	0	800	617.02		617.01975	800	617.01975	800
torsional shear	9504.1225		5520.25		3983.8753		15024.37	
torsional stress max at 45 deg	9504.1225		5520.25		3983.8753		15024.37	
bending stress		19008.245		11040.49		7967.75053		30048.7395
Principal 1	10474.611	19041.8552	18021.7	11240.49	18012.002	8245.36985	25855.089	29870.1655
Principal 2	-8623.5515	-33.610171	-1712.03	0	-902.2859	-77.61932	-8745.373	-21.426061
shear max	9549.0811	9537.73267	9866.89	5620.247	9457.1438	4161.49458	17300.231	14945.7958
moment	0	3271.2	2806.8	1900	2806.8	1371.2	2806.8	5171.2
torque	3271.2		1900		1371.2		5171.2	

Forces are listed in [lbf], stresses in [psi], and moments in [in-lbf]. As shown, the maximum stress is 29.9 [ksi]. This stress is well below the 75 [ksi] yield stress of 4130 Steel.

A6.3 FEA Check of Rear Suspension

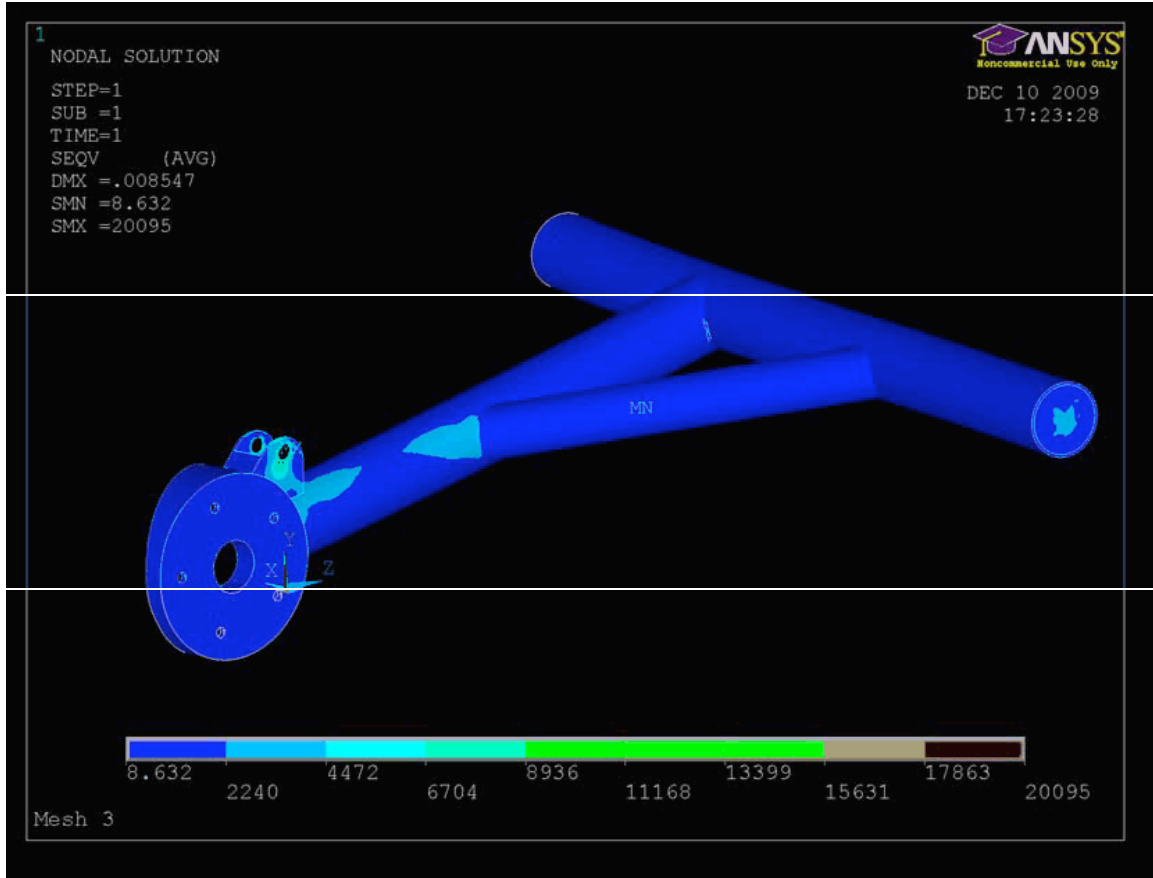


Figure A6.3 - ANSYS Investigation of Rear Suspension

The maximum stress in the rear suspension was determined to be 20 [ksi] from ANSYS simulation. This is also well below the rated stress for 4130 Steel.